ELSEVIER

Materials Science and Engineering A 483–484 (2008) 611–616

MATERIALS SCIENCE & ENGINEERING A

www.elsevier.com/locate/msea

Formation of dendritic nanostructures in Pyrex glass anodically bonded to silicon coated with an aluminum thin film

Yu-Qun Hu [a], Ya-Pu Zhao [a,*], Tongxi Yu [b]

[a] *State Key Laboratory of Nonlinear Mechanics (LNM), Institute of Mechanics, Chinese Academy of Sciences, Beijing 100080, People's Republic of China*

[b] *Department of Mechanical Engineering, Hong Kong University of Science and Technology, Clear Water Bay, Kowloon, Hong Kong, SAR, People's Republic of China*

Received 6 June 2006; received in revised form 20 September 2006; accepted 21 September 2006

Abstract

Anodic bonding with thin films of metal or alloy as an intermediate layer, finds increasing applications in micro/nanoelectromechanical systems. At the bonding temperature of 350 °C, voltage of 400 V, and 30 min duration, the anodic bonding is completed between Pyrex glass and crystalline silicon coated with an aluminum thin film with a thickness comprised between 50 and 230 nm. Sodium-depleted layers and dendritic nanostructures were observed in Pyrex 7740 glass adjacent to the bonding interface. The sodium depletion width does not increase remarkably with the thickness of aluminum film. The dendritic nanostructures result from aluminum diffusion into the Pyrex glass. This experimental research is expected to enhance the understanding of how the depletion layer and dendritic nanostructures affect the quality of anodic bonding.
© 2007 Elsevier B.V. All rights reserved.

Keywords: Anodic bonding; Dendritic nanostructures; Aluminum thin film; Depletion layer; MEMS

1. Introduction

Anodic bonding, also known as field-assisted bonding or electrostatic bonding [1], was developed as a method to bond metals, alloys or semiconductors to conductive glasses. This process has become an important technique in the semiconductor device industry, especially in the field of micro/nanoelectromechanical systems (MEMS/NEMS). It is also a highly promising method for joining certain metals or semiconductors to alkali ion-conductive glasses at decreased temperatures [2]. Compared to other techniques, the main advantage of anodic bonding is that a strong bond can be achieved at a reduced bonding temperature by application of an electric field [3]. The temperature for anodic bonding is usually lower than the softening point of glass and the melting points of the materials selected for this purpose. Currently, anodic bonding is used for making relatively simple devices [4], but there exists a demand for this straightforward and reliable bonding technique in connecting, packaging, or hermetic sealing of more complex micro/nanostructures and integrated microcircuits in MEMS/NEMS devices.

In the anodic bonding process, two perfectly planar and clean surfaces of two materials must be brought into close contact first. When the bonding temperature is reached, a direct current (dc) voltage is applied for a certain time. The conductive glass is on the cathode side, and the metal, alloy, or semiconductor on the anode side. Fig. 1 shows a schematic of anodic bonding between Pyrex 7740 glass and aluminum-coated crystalline silicon. Once a dc voltage is applied, the mobile cations in the glass, e.g. sodium cations, move away from the bonding interface to the cathode, creating a cation-depleted layer adjacent to this interface. The bonding surfaces are pressed into intimate contact by an electrostatic force in the electrical field due to the movement of the cations [5]. A permanent bond is believed to be formed by anodic oxidation of the anode material at the interface. The oxygen anions presumably originate from either the non-bridging oxygen (NBO) ions in the glass network or from the water dissolved in the glass surface [6–9].

Understanding the behavior of the interface during bonding is essential to obtain good (i.e. strong and sealed) bonds [4]. So far most of the studies on the bonding mechanism have dealt with the formation of intimate contact during the initial stage of

* Corresponding author.
E-mail address: yzhao@lnm.imech.ac.cn (Y.-P. Zhao).

0921-5093/$ – see front matter © 2007 Elsevier B.V. All rights reserved.
doi:10.1016/j.msea.2006.09.155

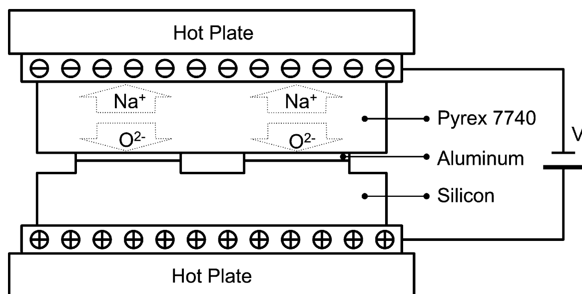

Fig. 1. Schematic of anodic bonding between Pyrex 7740 glass and aluminum-coated crystalline silicon.

bonding [5,10–12] and the formation of a cation-depleted layer [4,8,13–17] by bonding a variety of glasses to metals, alloys or semiconductor materials [18,19]. With the help of scanning electron microscopy (SEM) and transmission electron microscopy (TEM), the studies on the electrostatic bonding of Kovar and silicon to borosilicate glass [15], 0.5 mm thick Pyrex glass to 1 mm thick aluminum sheet [2], and 3 mm thick Pyrex glass to 0.5 mm thick aluminum sheet [4] have produced some interesting results.

To the authors' knowledge, no study has been reported on the nanostructures adjacent to the interface between Pyrex glass and aluminum-coated crystalline silicon anodically bonded at 350 °C and under 400 V. Bonding at both low temperature and low voltage can prevent the metal leads and integrated circuits in MEMS devices from degradation. A low bonding temperature can also minimize thermal stresses after cooling. van Helvoort et al. [4] reported that when the glass is bonded to a thick aluminum sheet at 450 °C and 1000 V during 15 min, some dendritic nanostructures form in the glass near the interface between the glass and the aluminum. They also pointed out twinned γ-Al_2O_3 in these dendritic nanostructures which are suggested, without further explanation, to act like nails, hooking the aluminum to the glass, thus contributing to the bonding quality. Aluminum is commonly considered a perfectly blocking anode material, that is, no aluminum cations from anode are pulled into glass during the bonding process, but recent studies [2,4] show aluminum diffusion into glass. No mechanism has been provided so far to account for the growth of these dendritic nanostructures. While most available studies focus on bonding configurations not relevant to practical MEMS/NEMS devices, anodic bonding with metal or alloy thin films finds increasing applications in the fabrication of MEMS/NEMS devices and provides a higher degree of freedom in MEMS/NEMS device design.

We have recently studied the anodic bonding between Pyrex 7740 glass wafer and crystalline silicon interlayered by a thin aluminum film, which will be used to anchor MEMS structures. This kind of anchor structure plays an important role in MEMS sensors (e.g. MEMS inertial micro-accelerometers). Usually, the anchor acts as mechanical or electrical connector between the mobile structures and the static substrate.

In this paper, we study depletion layers and dendritic nanostructures adjacent to the bonding interface between Pyrex glass and crystalline silicon coated with aluminum by scanning transmission electron microscopy (STEM) and TEM. The objective in this study is to provide a better understanding how the depletion layers and the dendritic nanostructures affect the quality of the anodic bonding at our bonding condition.

2. Experimental preparations

2.1. Anodic bonding

Pyrex 7740 glass wafers with 500 μm thickness and 100 mm diameter were cut into 12 mm × 12 mm square chips. Their chemical composition includes 80.8 mol% SiO_2, 12.0 mol% B_2O_3, 4.2 mol% Na_2O, 2.0 mol% Al_2O_3, 0.6 mol% K_2O, 0.2 mol% MgO, and 0.2 mol% CaO [20]. Si wafers of 100 mm in diameter (double-side polished; p-type; wafer surface plane (1 0 0)) were patterned into 4 mm × 4 mm mesas with 6 mm center-to-center spacing. The mesas, 10 μm in height, were prepared with a deep reactive ion etch (DRIE) process. The patterned Si wafers were coated by an ARC-12M sputtering system with pure aluminum (99.999%) at thicknesses of 500, 950, 1500, and 2300 Å, respectively. Then these Si wafers were also diced into squares of 12 mm × 12 mm. All square samples were cleaned by deionized water spray rinse in a 100-class clean room and dried by nitrogen gas under pressure. A pair of glass and well-coated crystalline silicon chip was placed between two stainless steel plates and then between two hot plates, which acted as plate electrodes. The glass was connected with the cathode side. The schematic of this bonding configuration is shown in Fig. 1. The bonding was performed at 350 °C and 400 V for 30 min on an open (non-vacuum) bonder. The bonding voltage was applied when the selected bonding temperature was reached. When the bonding was completed, the bonded sample was cooled to room temperature of 20 °C in 2 h.

2.2. Transmission electron microscopy

To prepare TEM specimens, the bonded samples were cut into small bars with a cross-section of 1.5 mm × 1.5 mm (perpendicular to the interface). These bars were glued into 3 mm diameter copper tubes with an inner diameter of 2.2 mm. The copper tubes were sectioned into slices approximately 750 μm thick, and then ground down to a thickness of about 40 μm and dimpled at the interface. Before argon-ion milling, these foils were attached to molybdenum support rings with an inner diameter of 1 mm. Specimens were ion milled to electron transparency at room temperature by a Gatan Model 691 precision ion polishing system (PIPS).

All specimens were examined in a 300 kV Tecnai F30 (FEI Field Emission Gun TEM with LaB_6 filament). STEM and energy dispersive X-ray (EDX) spectroscopy microanalysis were used for chemical analysis.

3. Results and discussion

3.1. Depletion layer

All samples, bonded at 350 °C, 400 V, and during 30 min, showed good bonds. Optical microscopy at a magnification ×50 revealed were cracks neither in the Pyrex glass nor in the crys-

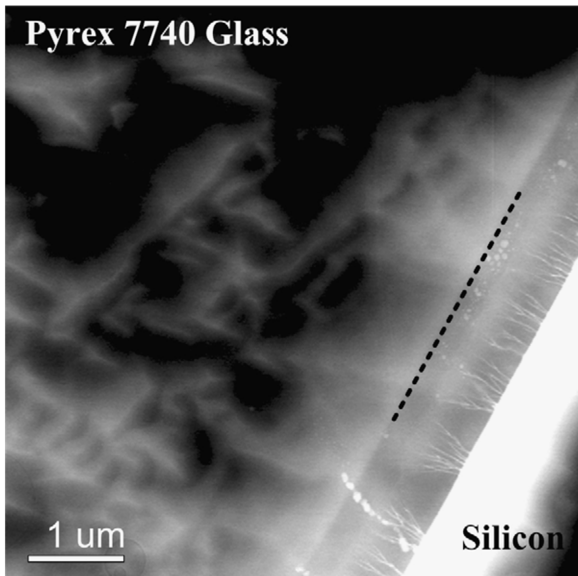

Fig. 2. The typical TEM and STEM images of sodium depletion layer. The short black dotted line underlines (emphasizes) the edge of sodium depletion layer.

talline silicon, and this was subsequently confirmed by TEM. The small bars survived the cutting force of the dicing machines without debonding which proves that the bonding of the samples is strong enough to withstand the mechanical cutting force.

STEM images show a distinguishable layer in the Pyrex glass adjacent to the Al/glass interface (Fig. 2). This is the sodium-depleted layer, which has a width of 800–900 nm that can also be observed in bright-field TEM images. With mobility higher than that of the other cations, the sodium cations (Na^+) in Pyrex 7740 glass wafers are the main cations migrating during the formation of this depletion layer. Other alkali cations, such as potassium (K^+) and calcium (Ca^{2+}), were also found to contribute in the depletion layer [8,14,21,22]. In Fig. 2, a short black dotted line schematically marks out the edge of the depletion layer. The potassium cations are aggregated in the darker band at this edge. The sodium depletion widths listed in Table 1 are averaged from four or more different positions. Clearly, the sodium depletion width does not change remarkably with the change of the thickness of the aluminum thin film.

3.2. Dendritic nanostructures

In all anodically bonded samples, dendritic nanostructures were found in the Pyrex glass near the Al/glass interface (Fig. 3). The aluminum film thicknesses in Fig. 3a–d are 500, 950, 1500, and 2300 Å, respectively. The dendritic nanostructures, which are seen over the whole thin area, exhibit a similar maximum height of 600–650 nm in the specimens bonded during 30 min at 350 °C, 400 V. These three-dimensional treelike structures have a trunk a few tens of nanometers in diameter (less than 40 nm). All the dendritic structures grow in the sodium depletion layer from the Al/glass interface to the bottom of potassium-aggregated band. Obviously, TEM cannot show all the small branches of these three-dimensional nanodendritic structures.

Table 1
The sodium depletion layer width in glass/Al/Si anodic bonding at 350 °C, 400 V during 30 min

Sample group number	Thickness of Al film (nm)	Sodium depletion layer width (nm)
1	50	871
2	95	870
3	150	875
4	230	882

Figs. 4 and 5 illustrate the EDX analysis of the nanodendritic structures under STEM mode. The electron beam scanning path is marked with a black thick line across three trunks of the dendritic structures (Fig. 4). Element analysis indicates that the dendritic nanostructures are aluminum enriched (Fig. 5). STEM/EDX microanalysis provides convincing evidence of aluminum having diffused into the Pyrex glass during anodic bonding. The bottom count curve in Fig. 5 indicates that the band adjacent to the glass/Al interface is of sodium depleted. Examined by EDX, the trunks exhibit lesser counts of silicon and oxygen while the aluminum counts are conspicuously increased.

Fig. 6 shows typical nano-crystals grown in the trunk of a dendritic structure, along with computed fast Fourier transforms (FFTs) of the lattice image of the crystallized area. The interplanar spacing has amounts to 0.273 nm.

3.3. Discussion

It is commonly assumed that thermal fields and assisted electric fields are responsible for the activation of ions and the drift during an anodic bonding process. In the glass, oxygen usually exists in the forms of $[SiO_4]^-$, $[BO_4]^-$, $[AlO_4]^-$, contributing to the glass-network formation. But the oxygen belonging to –O–Na bonds is not responsible for the glass-network formation and behaves in a more mobile way than oxygen under other forms under an external field [2]. This form is called NBO and it is weakly bonded in the glass matrix.

Due to the low thermal activation energies of alkali ions in Pyrex glasses, when unbonded samples are heated to the bonding temperature and the bonding voltage is applied, mobile cations, mainly sodium cations, drift from the Pyrex glass region near the aluminum to the negatively charged cathode through the bulk glass. The migration of sodium cations forms the sodium depletion layer in the Pyrex glass adjacent to the glass/Al interface. At the same time, the negative space charges, NBO ions, drift towards the interface, and are accumulated over the depletion region. Therefore, at the interface, some chemical reaction occurs between these NBO anions and aluminum, and this is how the bonding takes place.

Under these circumstances, the amount of migrating ions increases with the bonding temperature and voltage, which leads to more anions accumulated in the depleted layer, and to the thickening of the depletion layer. The electrostatic field across the bonding interface is accordingly increased, which brings about much larger and more intimate contact area between the Pyrex glass and aluminum, that is, more chemical bonds generated at the bonding interface and an improvement of the bonding. However, a high bonding voltage will introduce a risk of electric

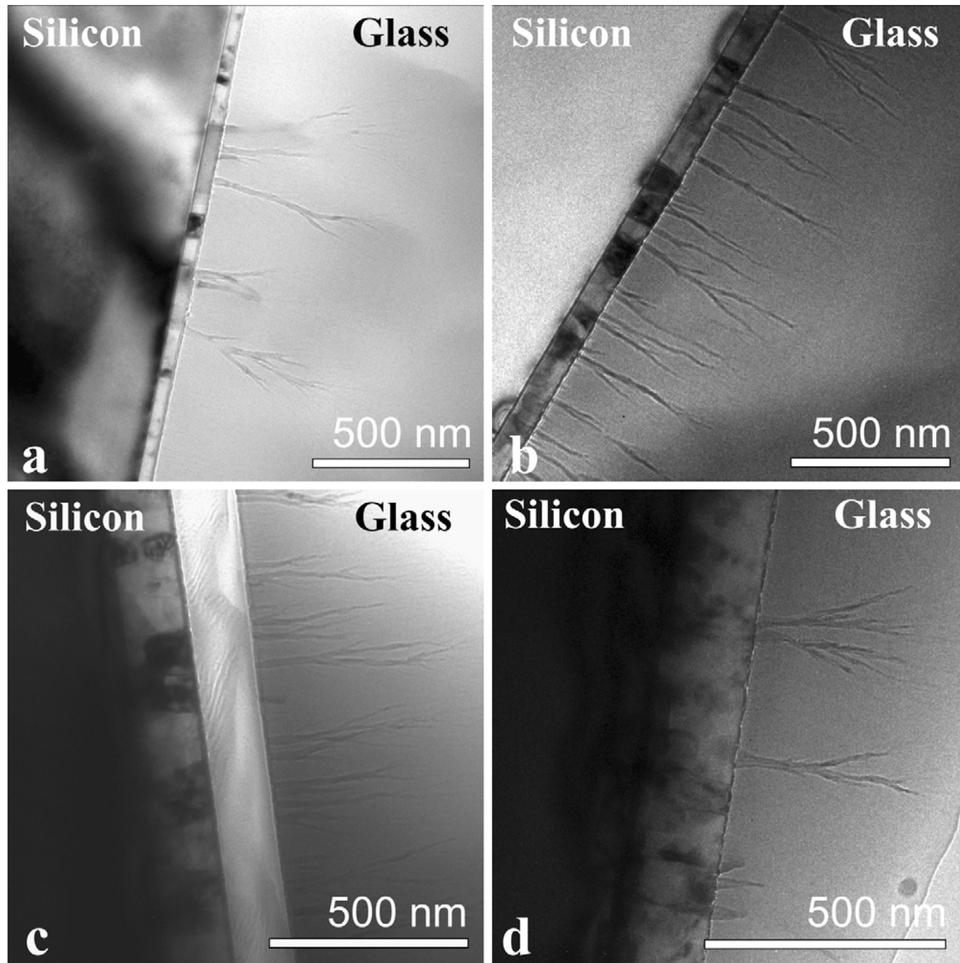

Fig. 3. Bright-field TEM images of dendritic nanostructures of specimens with: (a) 50 nm, (b) 95 nm, (c) 150 nm, and (d) 230 nm aluminum thin film, bonded 30 min at 350 °C, under 400 V.

breakdown. In the same vein, a high bonding temperature may not only deteriorate metal leads and integrated circuits in MEMS device, but it may also introduce large thermal stresses. It is in fact because we found some cracks in glass due to thermal stress in earlier bonding experiments that a low bonding temperature of 350 °C and a voltage of 400 V were selected in the present study.

According to our experimental results, the depletion layer reaches a saturation thickness for sufficiently long bonding durations. A typical bonding current–time curve is shown in Fig. 7. When the bonding time exceeds the duration time corresponding to saturation, the bonding current reduction is no longer signif-

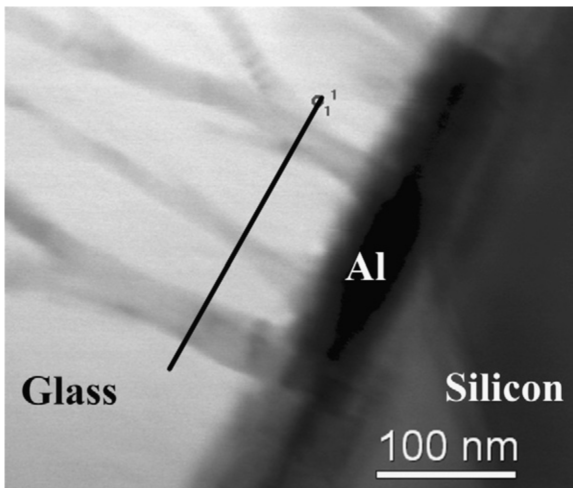

Fig. 4. Scanning position in STEM mode for EDX analysis.

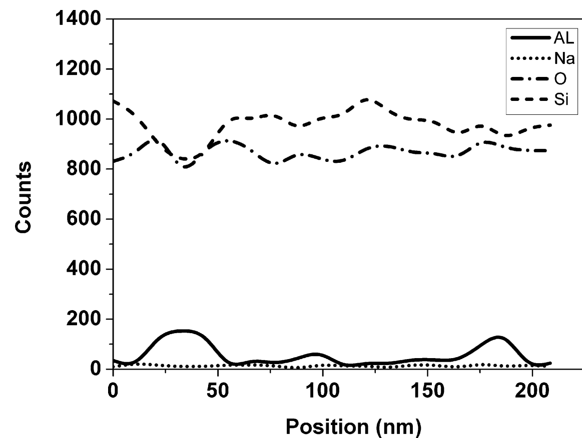

Fig. 5. EDX analysis for element counting in STEM mode.

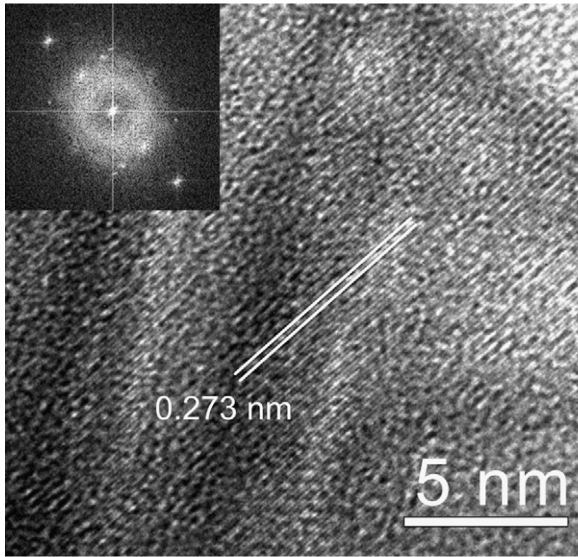

Fig. 6. High-resolution TEM images of the dendritic nanostructure in Pyrex glass after anodic bonding.

icant, that is, the sodium depletion layers in samples cease to grow and reach their saturation widths. The experimental results in Table 1 also suppose that, under the same bonding temperature and voltage, the same widths of depletion layer will be acquired in agreement with the results of Nitzsche et al. [8] and van Helvoort et al. [9], however, from another reasoning.

In order to estimate the sodium depletion width d, the following formulae are suggested in references [8,14,21,22],

$$d = \frac{Q}{A\rho e} \quad \text{and} \quad Q = \int_0^T I(t)\mathrm{d}t,$$

where I is the current of bonding, A the bonding area on specimen, ρ the sodium ion density ($1.49 \times 10^{18}\ \mathrm{mm}^{-3}$), e is the elementary charge (1.6×10^{-19} C), and T is the bonding time. We find that, for a long time bonding (1800 s), the widths of the depletion layers estimated from these equations deviate substantially from those measured on TEM/STEM images. It is only for the bonding within the saturation time that the depletion widths estimated by these equations agree with our results. In the case of samples in group 1 (Table 1), it takes 49.4 s to reach the saturation width for sodium depletion, as shown in Fig. 7.

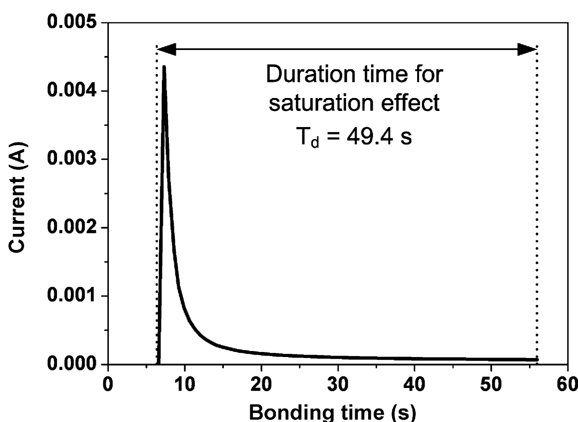

Fig. 7. The bonding current and the duration time for the saturation effect of sodium depletion.

The depletion layer plays an important role in the formation of a successful anodic bonding. It is the negative space charges in the depletion layer that induces a high-intensity electric field across the interface. The large electric field force forces the bonding surfaces into intimate contact, accommodating the imperfections such as roughness and very small particles, by elastic, plastic, and viscous deformations of the glass [5].

High-resolution TEM images (Fig. 6) demonstrate that there are many crystallized areas in the dendritic nanostructures. Due to the fact that the lattice planes are superimposed by the glass-substrate, those white spots in the FFT image comprise some amorphous character. Unfortunately, because of aperture limitations, selected area diffraction (SAD) patterns of the dendritic nanostructures could not provide enough information to distinguish these nano-crystals, but according to the previous STEM results, and considering that the NBO ions in the glass are the main anions migrating toward the glass/Al interface at 350 °C (far less than the transition point of Pyrex glass), these crystallized areas in the dendritic structures must be the crystalline compound formed after the chemical reactions between the NBO anions and aluminum ions. Based on this mechanism, the dendritic nanostructures would only grow in the sodium depletion layer with a height less than the sodium-depleted width in Pyrex glass. van Helvoort et al. [4] claimed that at 450 °C aluminum in the glass was present primarily in the form of γ-Al_2O_3, but they did not make the glass/Al-coated Si anodic bonding under the conditions used in this study. However, their results provide a helpful clue for analyzing these nano-crystals.

Wallis and Pomerantz [1] pointed out that, at the beginning of a bonding process, the bonding voltage is distributed uniformly along the thickness of the glass, and as the space charge is accumulated near the interface, an increasingly large part of the total voltage is developed across this thin depletion layer. Consequently, high-intensity electrostatic fields are generated adjacent to the Al/glass interface. However, Wallis et al. did not mention the distribution of electrostatic fields in the plane of the bonding interface. To explain why the aluminum diffuse into the glass in the form shown in Fig. 3, we believe that the following argument must be considered. The real bonding surfaces, which exhibit micro or nanoscale roughness and non-planarity, are not ideal, perfectly planar and clean planes. At the very beginning, the contact between the bonding surfaces only occurs at a few isolated points. Therefore, during the bonding process, the interfacial electrostatic fields are not uniformly distributed along the glass/Al interface. The aluminum will diffuse into glass more easily from the interface region with higher field intensity, due to the non-uniform distribution of space charges in the Pyrex glass. On the other hand, a larger gradient of local electrostatic field results in a higher diffusion rate and a larger diffusion depth for the aluminum in intimate contact with the Pyrex glass. Spatial non-uniform electrostatic fields are of key importance for the growth of the dendritic nanostructures from the glass/Al interface. The growth of the dendritic nanostructures is a non-

equilibrium growth process, and these nanostructures have a typical three-dimensional fractal shape.

For the specimens bonded in this study, TEM shows that aluminum diffuses into the Pyrex glass notably in the form of a dendritic, indicating in turn that it is a not so perfect blocking anode material. The diffusion of aluminum into Pyrex glass increases the amount of chemical bonds between the Pyrex glass and the aluminum film, and increases the bonding strength. After anodic bonding, the aluminum thin film takes root in the Pyrex glass by means of dendritic crystallized nanostructures, just as a tree roots in ground.

Due to the quite low diffusion velocities of aluminum and the relative immobility of the NBO anions, the diffused aluminum cations cannot neutralize all of the anions in the depletion layer and there are still many space charges in the depletion region [2]. These residual space charges also generate a considerable attraction force across the interface after bonding.

4. Conclusion

Pyrex 7740 glass and crystalline silicon coated with thin aluminum film maintained 30 min at 350 °C, under a voltage of 400 V transform into anodically bonded samples with good bonds which resist dicing.

The presently designed anodic bonding process generates a sodium depletion layer about 800–900 nm thick in Pyrex 7740 glass, adjacent to the Al/glass interface. The widths of the sodium-depleted regions do not increase remarkably with the thickness of the aluminum thin film used in this work (50–230 nm). Higher temperature and voltage may increase the sodium depletion width in Pyrex 7740 glass, and then improve the bonding strength, however, at the risk of failure of the MEMS devices. The sodium depletion layers attain a saturation thickness for a long bonding time. It is in the saturation stage that the widths of the depletion layers increase with the bonding temperature, voltage, and time (if it is saturated it cannot increase with time).

The formation of the dendritic nanostructures is due to the diffusion and reaction near the glass/Al interface under a non-equilibrium condition during the anodic bonding process. These nanostructures might reveal helpful in improving the bonding quality. The heights of these fractal structures are limited by the sodium depletion width. The dendritic nano-crystalline structures are shown to be one of the key structures for the improvement of strength in anodic bonding. In addition, aluminum is not a perfectly blocking anode material under the bonding condition of this study.

Acknowledgements

We would like to thank Mr. Wan Lap Yeung of Hong Kong University of Science and Technology and Ms. Xiaoping Zhang of Peking University for their help during experiments and TEM observation. This work was supported by the National Natural Science Foundation of China (NSFC) (grant No. 10225209 and No. 90305020), key project from the Chinese Academy of Sciences (grant No. KJCX2-SW-L2), and NSFC-RGC Joint Project (grant No. 50131160739).

References

[1] G. Wallis, D.I. Pomerantz, J. Appl. Phys. 40 (1969) 3946–3949.
[2] Q. Xing, G. Sasaki, H. Fukunaga, J. Mater. Sci.: Mater. Electron. 13 (2002) 83–88.
[3] J. van Elp, P.T.M. Giesen, J.J. van der Velde, J. Vac. Sci. Technol. B 23 (2005) 96–98.
[4] A.T.J. van Helvoort, K.M. Knowles, J.A. Fernie, J. Am. Ceram. Soc. 86 (2003) 1773–1776.
[5] T.R. Anthony, J. Appl. Phys. 54 (1983) 2419–2428.
[6] T.T. Veenstra, J.W. Berenschot, J.G.E. Gardeniers, R.G.P. Sanders, M.C. Elwenspoek, A. van den Berg, J. Electrochem. Soc. 148 (2001) G68–G72.
[7] S. Mack, H. Baumann, U. Gosele, H. Werner, R. Schlogl, J. Electrochem. Soc. 144 (1997) 1106–1111.
[8] P. Nitzsche, K. Lange, B. Schmidt, S. Grigull, U. Kreissig, B. Thomas, K. Herzog, J. Electrochem. Soc. 145 (1998) 1755–1762.
[9] A.T.J. van Helvoort, K.M. Knowles, J.A. Fernie, J. Electrochem. Soc. 150 (2003) G624–G629.
[10] K.B. Albaugh, D.H. Rasmussen, J. Am. Ceram. Soc. 75 (1992) 2644–2648.
[11] T.M.H. Lee, D.H.Y. Lee, C.Y.N. Liaw, A.I.K. Lao, I.M. Hsing, Sens. Actuators A 86 (2000) 103–107.
[12] M.A. Morsy, K. Ikeuchi, M. Ushio, H. Abe, Mater. Trans. JIM 37 (1996) 1511–1517.
[13] M.P. Borom, J. Am. Ceram. Soc. 56 (1973) 254–257.
[14] D.E. Carlson, K.W. Hang, G.F. Stockdale, J. Am. Ceram. Soc. 57 (1974) 291–300.
[15] M.A. Morsy, K. Ikeuchi, M. Takahashi, M. Ushio, ASM International, Pine Mountain, GA, US, 1998, pp. 251–256.
[16] B. Schmidt, P. Nitzsche, S. Grigull, U. Kreissig, B. Thomas, K. Herzog, K. Lange, Sens. Actuators A 67 (1998) 191–198.
[17] A.T.J. van Helvoort, K.M. Knowles, C.B. Boothroyd, J.A. Fernie, Transmission electron microscopy of silicon-Pyrex electrostatic bonds, in: M. Aindow, C.J. Kiely (Eds.), Electron Microscopy and Analysis, IOP Publishing Ltd., Bristol, 2001, pp. 341–344.
[18] W.H. Ko, J.T. Suminto, G.J. Yeh, Bonding Techniques for Microsensors, Elsevier, Amsterdam, 1985, pp. 41–61.
[19] C. Tudryn, S. Schweizer, R. Hopkins, L. Hobbs, A.J. Garratt-Reed, J. Electrochem. Soc. 152 (2005) E131–E134.
[20] J.E. Shelby, J. Appl. Phys. 51 (1980) 2561–2565.
[21] D.E. Carlson, K.W. Hang, G.F. Stockdale, J. Am. Ceram. Soc. 55 (1972) 337–341.
[22] C.M. Lepienski, J.A. Giacometti, G.F.L. Ferreira Jr, F.L. Freire, C.A. Achete, J. Non-Cryst. Solids 159 (1993) 204–212.